The CRISTA-2 mission

K. U. Grossmann, D. Offermann, O. Gusev, J. Oberheide,[1] M. Riese,[2] and R. Spang[3]
Physics Department, University of Wuppertal, Wuppertal, Germany

Received 23 March 2001; revised 7 November 2001; accepted 10 November 2001; published 25 October 2002.

[1] The second mission of the *CR*yogenic *I*nfrared *S*pectrometers and *T*elescopes for the *A*tmosphere (CRISTA) experiment took place in August 1997. The experiment was flown aboard the *ASTRO*nomical *S*huttle *PA*llet *S*atellite (ASTRO-SPAS) free-flying platform launched by the NASA space shuttle. CRISTA analyzes the infrared radiation emitted by trace gases from the Earth limb in the altitude regime from the upper troposphere to the lower thermosphere. The main aim of CRISTA is to detect small-scale dynamically induced structures in the distribution of trace constituents in the middle atmosphere. The instrument is therefore equipped with three telescopes that simultaneously collect the infrared radiation from three different air volumes. The high spatial density of the measurement grid obtained during the first CRISTA mission in November 1994, as well as the latitudinal coverage, was considerably improved by making use of newly developed satellite pointing and maneuvering capabilities. The altitude coverage was extended to include the upper troposphere where water vapor distributions are analyzed. Dynamically induced features are observed in practically all trace gases and at various spatial scales. The smallest scales that could be analyzed on the basis of the CRISTA data set are well below 100 km. Compared to the first mission, much more emphasis was laid on measurements in the upper mesosphere and lower thermosphere—this was possible because of higher radiometric sensitivities in some channels. Atomic oxygen, carbon dioxide, and ozone densities are derived in the upper mesosphere and lower thermosphere. The mission conditions allowed the study of polar stratospheric clouds (PSC) over the Antarctic and of polar mesospheric clouds (PMC) at high northern latitudes. For the first time, summer high latitude mesopause temperatures were retrieved from CO_2 15-μm spectra using a nonlocal thermodynamic equilibrium model. The derived temperatures compare well with a temperature climatology based on rocket soundings. *INDEX TERMS:* 0341 Atmospheric Composition and Structure: Middle atmosphere—constituent transport and chemistry (3334); 0342 Atmospheric Composition and Structure: Middle atmosphere—energy deposition; 0350 Atmospheric Composition and Structure: Pressure, density, and temperature; 0394 Atmospheric Composition and Structure: Instruments and techniques

Citation: Grossmann, K. U., D. Offermann, O. Gusev, J. Oberheide, M. Riese, and R. Spang, The CRISTA-2 mission, *J. Geophys. Res.*, *107*(D23), 8173, doi:10.1029/2001JD000667, 2002.

1. Introduction

[2] For a long time most properties of the Earth's middle atmosphere were characterized by zonal mean values or even by spatial and temporal constants. Later it became evident on the basis of experimental data that large scale planetary waves modulate important stratospheric parameters, including temperature and ozone concentration [*Drummond et al.*, 1980; *Krueger et al.*, 1980; *Gille and Russell III*, 1984]. Experiments carried out from the ground, on balloons, or by sounding rockets frequently revealed atmospheric variability on much smaller scales and in practically all atmospheric parameters and at all altitudes. Some examples of such structures are found in the studies of *Offermann* [1987], *Murphy et al.* [1993], *Pfister et al.* [1993], and *Thrane et al.* [1994]. The observed small- and medium-scale structures are mostly due to dynamical processes. Quantitative knowledge of winds, waves, or turbulence is of considerable interest, as part of the trace gas and energy transport in the atmosphere occurs via these processes [*McIntyre and Palmer*, 1983; *Randel et al.*, 1993; *Chen et al.*, 1994]. Previous development of measuring techniques has led to important improvements in simultaneous coverage of many trace gases, as well as in measurement precision and accuracy. The spatial and temporal measurement density has, however, not been augmented in a similar way [*Grossmann*, 2000]. As numerical models go to higher and higher spatial resolution, the

[1]Now at High Altitude Observatory, National Center for Atmospheric Research, Boulder, Colorado, USA.
[2]Now at Institute for Chemistry and Dynamics of the Geosphere, Institute I: Stratosphere, Research Center Jülich, Jülich, Germany.
[3]Now at Department of Physics and Astronomy, University of Leicester, Leicester, UK.

Copyright 2002 by the American Geophysical Union.
0148-0227/02/2001JD000667

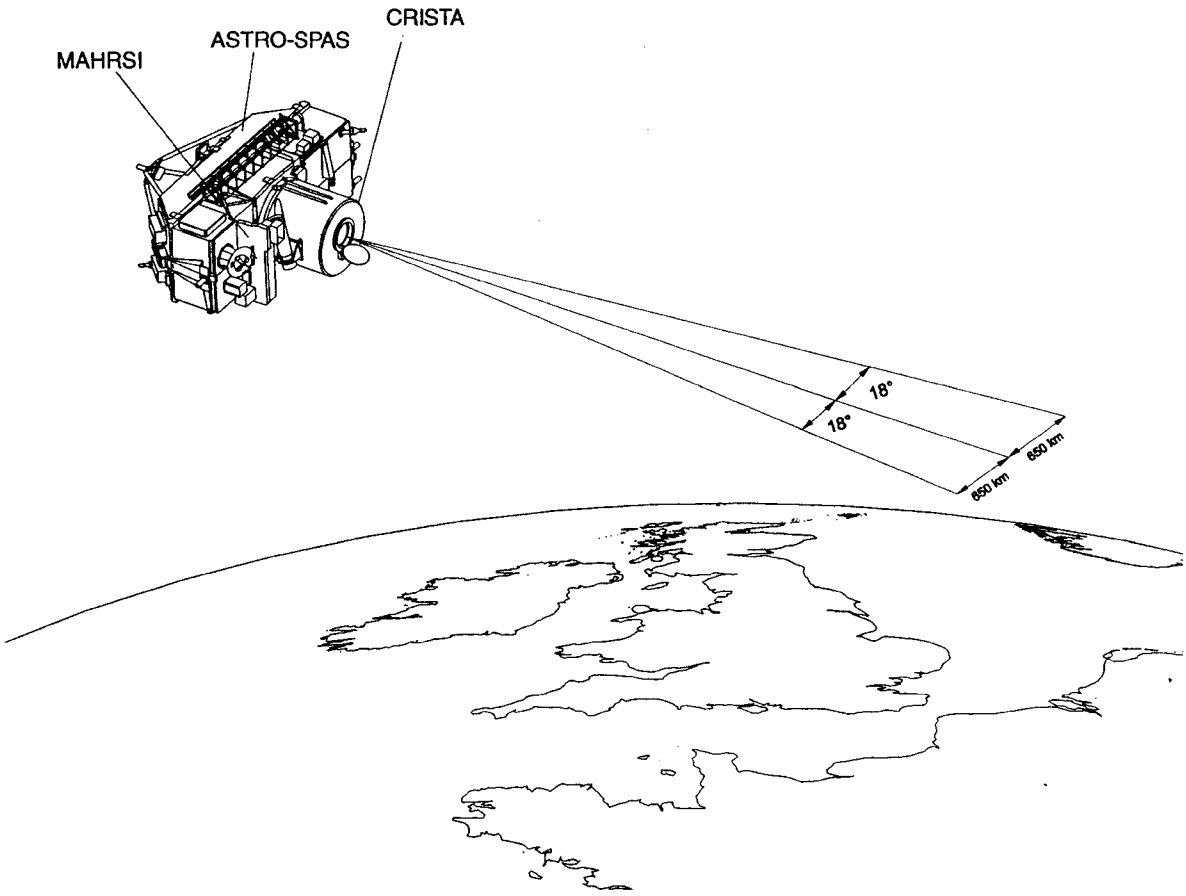

Figure 1. The CRISTA measurement geometry.

demand for high spatial density global information increases. Studies of middle atmospheric composition or dynamics on a global scale require satellite remote sensing measurements. Infrared or microwave sounders can sense the atmosphere at all local times, independent of solar illumination. Basically two types of observation geometry are used. The limb sounders exhibit a good vertical resolution, on the order of 1–2 km, but their horizontal data density is generally poor because it is limited by the separation of two successive orbits. Nadir sounders in contrast have a very good horizontal resolution, which in some cases is combined with imaging or cross-track scanning, yielding a very dense data network. Their vertical resolution is, however, poor or even restricted to total column measurements.

[3] An important step toward improving the spatial data density in all three dimensions, combined with good temporal resolution for a large number of trace gases, has been achieved with the triple telescope sensor CRISTA (*CR*yogenic *I*nfrared *S*pectrometers and *T*elescopes for the *A*tmosphere). CRISTA is a cryogenically cooled infrared limb sounding instrument optimized to measure trace gases in the middle atmosphere on a dense horizontal grid. This is achieved by using three independent telescopes each followed by grating spectrometers for the midinfrared spectral regime. The three telescopes (called L, C, and R for *l*eft, *c*enter, and *r*ight, respectively) simultaneously sense three atmospheric volumes separated by 18° in azimuth. The three tracks of the CRISTA instrument are separated by about 650 km at the tangent point in the stratosphere, in the case when the main axis of the instrument (which is the center telescope viewing direction) lies in the orbital plane. The measurement geometry is sketched in Figure 1. The distance between two air volumes along the orbital flight direction is a function of the time needed to perform one altitude scan and is between 200 and 600 km except for some special observation modes.

[4] For its orbital measurements CRISTA is integrated in the free-flying science platform ASTRO-SPAS (*ASTRO*nomical *S*huttle *PA*llet *S*atellite [*Wattenbach and Moritz*, 1997]) which is launched and subsequently retrieved by the NASA space shuttle for short-lived exploratory missions. Jointly with the CRISTA infrared soundings, ultraviolet spectra are measured by the *M*iddle *A*tmosphere *H*igh *R*esolution *S*pectrograph *I*nvestigation (MAHRSI [*Conway et al.*, 1999]). MAHRSI is bore-sighted with the central CRISTA telescope.

[5] The first flight of CRISTA was part of the space shuttle mission STS 66 together with the ATLAS-3 payload [*Kaye and Miller*, 1996] in November 1994. Details of this mission, as well as a description of the instrument, are found in the work of *Offermann et al.* [1999]. The utility of the high data density obtained in the stratosphere and mesosphere was demonstrated during this flight. Structures of various scales, ranging from gravity waves to planetary scale disturbances, were detected in a number of trace gases

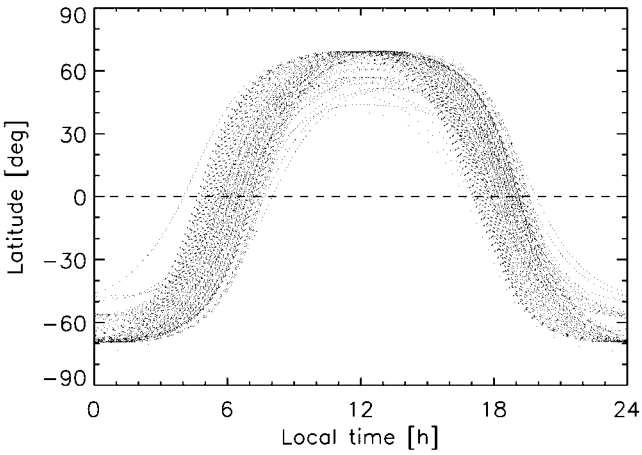

Figure 2. Distribution of the local times of the measured air volumes during the mission.

and were published in a series of papers referenced by *Offermann and Conway* [1999]. Further results are found in the studies of *Eckermann and Preusse* [1999], *Edwards et al.* [2000], *Oberheide et al.* [2000], *Preusse et al.* [2000], *Riese et al.* [2000, 2001], and *Tan and Eckermann* [2000].

[6] A different situation is encountered at higher altitudes. Most previous experimental efforts to measure trace gases have been devoted to the stratosphere so far. Little experimental data is available in the mesosphere and lower thermosphere, since few satellite experiments have been dedicated to this regime. Many parameters and many processes can be studied or are detected more easily at the higher altitudes since atmospheric chemistry is much simpler than in the stratosphere. Global climate change due to enhanced greenhouse gases are probably observed with much higher amplitudes in the mesosphere than below [*Beig*, 2000]. Some indications of long-term trends have been found in the appearance frequency of polar mesospheric clouds [*Gadsden*, 1997]. Although this altitude regime appears to be much simpler, a number of important questions remain open: these include the mesospheric ozone budget and the high water vapor mixing ratios detected in the vicinity of 70 km [*Crutzen*, 1997].The mesosphere can also have a considerable influence on the underlying layers via the so-called downward control principle [*Haynes*, 1991]. The high-latitude, zonally symmetric modulation known as the Arctic Oscillation (or Annular Mode) can propagate downward from the mesosphere to the stratosphere or even into the troposphere in some cases [*Baldwin and Dunkerton*, 1999, 2000]. A sufficiently well spatially resolved sounding of the mesosphere/lower thermosphere is thus very important for a future, more precise understanding of this region. A large part of the measurement time of CRISTA-2 was therefore devoted to the mesosphere and the lower thermosphere and the radiometric sensitivity of the relevant channels was enhanced.

2. The CRISTA-2 Experiment

[7] CRISTA on ASTRO-SPAS (also-called CRISTA-SPAS-2) was launched on 7 August 1997, at 1441 UT by space shuttle Discovery (mission STS 85) into its preplanned 300 km circular orbit with a 57° inclination. The ASTRO-SPAS satellite was released about 8 hours later for slightly less than 9 days of free flight. The northernmost point of the orbit was reached at about 1500 UT corresponding to about 1400 LST. Measurements were made between 8 August and 16 August. During this period the orbital plane precessed only by slightly more than 30°, so there was only a small change of about 2 hours in the local measurement times over the entire mission. The individual local times at the sensed air volumes vary to some extent due to the attitude of the satellite. The local times of the CRISTA center telescope tangent point for the complete mission are shown in Figure 2. The northern hemisphere was sensed essentially during daytime and the southern hemisphere during darkness. Mid and low latitude data are confined to the morning and evening hours. CRISTA-2 encountered two extreme atmospheric conditions—the cold sunlit summer mesopause in the north and the cold stratospheric night near and over the Antarctic, characterized by observations of polar mesospheric clouds (PMC) [*Stevens et al.*, 2001] as well as of polar stratospheric clouds (PSC) [*Spang et al.*, 2001]. For this second flight significant improvements were introduced to the instrument as well as the spacecraft, without changing the instrumental concept [*Grossmann and Offermann*, 1999]. As in the first mission, the MAHRSI experiment formed part of the scientific instrumentation of the ASTRO-SPAS.

[8] The main changes on the instrument hardware side are a replacement of the midinfrared Si:Ga detectors of the center telescope spectrometers (SCS and SCL) by Si:As BIB detectors [*Reynolds et al.*, 1989]. This increased the signal-to-noise ratio for most channels. The instrument performance in the upper mesosphere and lower thermosphere was thus improved in the center telescope. A further change was also made to the far-infrared spectrometer. A channel was added to measure the atomic oxygen emission line at 63 μm in the lower thermosphere; no absorbing filters

Table 1. Channel Allocation

Number	Species	Channel Designation[a]	Wavelength Coverage[b], μm
1	CH_4, N_2O, N_2O_5, CF_4	SL1, SCS1, SR1	7.5–8.6 [9.7]
2	CO_2, CO, O_3	SCS2	4.18–4.81 [5.36]
3	O_3	SL3, SCS3, SR3	8.91–10.22 [11.32]
4	NO, H_2O	SCS4, SR4	4.92–5.58 [6.13]
5	HNO_3, CFC12	SL4, SCS5, SR5	10.43–11.78 [12.88]
6	T, O_3, CFC11, HNO_3, $ClONO_2$, CCl_4	SL5, SCS6[c], SR6	11.55–12.88 [13.98]
7	H_2O, NO_2	SL6, SCS7, SR7	6.07–6.73 [7.28]
8	T, p	SL8, SCS8, SR8	12.79–14.1 [15.2]
10	O_3	SCL1	9.29–10.3
11	T, p	SCL2	14.34–15.58
12	$O(^3P)$, HF, H_2O	SCL3	59.0–65.0
13	N_2O, CO_2	SCL4	16.21–17.42
14	$O(^3P)$, HF, H_2O	SCL5	60.1–66.1
15	H_2O, HCl	SCL6	65.0–70.91

[a] SL, SR, SCS, SCL designate channels in the left, right, center short-wavelength, and center long-wavelength spectrometers, respectively.

[b] The wavelength limits given in brackets are for every 4th or 6th scan in the stratosphere or mesosphere modes, respectively.

[c] Two additional detectors are integrated in this channel: SCS6L and SCS6R which are used in conjunction with the special observation mode "staring" (Table 3) only.

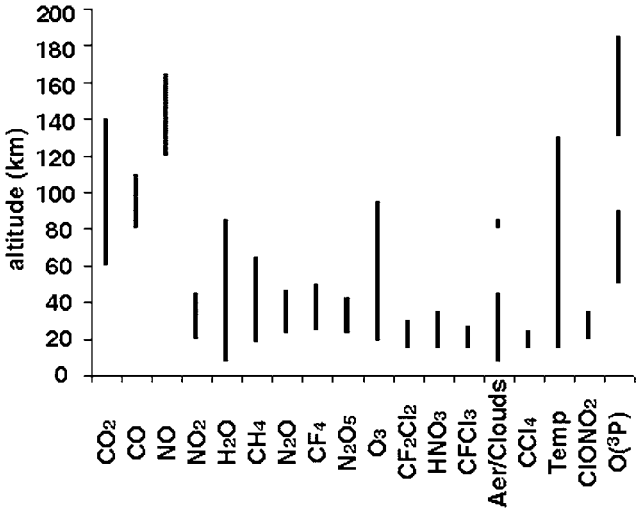

Figure 3. Gases analyzed by CRISTA-2.

are necessary as the 63 μm line is the only emission of importance at these altitudes and in this wavelength region. The signal-to-noise ratio was thereby increased by a factor of 10 compared to the capabilities of CRISTA-1. The scan range of each detector channel as used in CRISTA-2 and the species observed are summarized in Table 1. The altitudes at which trace gas densities and temperatures are (or will be) available from CRISTA-2 are shown schematically in Figure 3. In addition to the gases shown, emission features of HF, HCl, and HNO_4 have been identified.

[9] CRISTA was extensively calibrated before and after the mission. The radiometric sensitivity was determined using a large cryogenic blackbody which fills the complete field of view of CRISTA. Its temperature could be varied from 10 K to 260 K, covering the large wavelength range of CRISTA of 4–71 μm. During the course of the mission the temperatures of the SCS and SCL detectors changed, respectively, from 3.35 to 3.60 K and 3.28 to 3.51 K. All calibrations were therefore done for a series of discrete detector temperatures within this range. During the mission the relative sensitivity was monitored by viewing a blackened spot located on the inside of the instrument cover. This was done whenever the cover was closed. The absolute radiometric calibrations before and after the mission agreed to better than ±1% for most channels. In some cases the agreement is less good, it reaches only ±4.3% for the short wavelength BIB detectors (SCS2 and SCS4, Table 1). The relative sensitivity variations seen during the mission are similar (mostly <1% and <4.5% at maximum).

[10] In several cases the very high impedance photoconducting detectors in CRISTA show memory effects such that the instantaneous detector signal is influenced by the signal history over some preceding period. These relaxation effects vary between detectors and depend on the detector temperature. They generally reach a few % during calibration and in flight, but can be larger in extreme cases. Much effort was devoted to the characterization and quantification of the relaxation effects during ground calibration. A special cryogenic blackbody source was developed which allowed illumination of the detectors with pulses of a multitude of radiation levels and of varying lengths. Based on these measurements a correction model was developed [*Ern et al.*, 2002] which was successfully applied to the CRISTA-1 data set but which is still under development for CRISTA-2. To date, only a first-approximation correction has been applied to the CRISTA-2 data. The further effects of the application of the correction model are included in the present error estimates. The spectral resolution and the wavelength allocation was characterized by placing gas absorption cells in the telescope beams. The final adjustment of these parameters was made with the flight data from the atmosphere. The line of sight of the telescopes was measured and aligned relative to both the ASTRO-SPAS attitude reference and the MAHRSI instrument. In the mission, the line of sight calibration was verified twice by pointing CRISTA toward Jupiter while measuring reference star positions with the ASTRO-SPAS star camera.

[11] A major advance was made in the performance of the ASTRO-SPAS platform. The attitude of the satellite is derived from a star field camera and a gyro package in combination with a GPS (global positioning system) position determination. The attitude is actively controlled via a cold-gas system. For the second CRISTA mission a new attitude control software was available; this allowed the satellite to be slewed around the local vertical axis, while maintaining the fields of view of all three telescopes at the Earth's limb. The attitude timeline could be changed by ground commands in near real time. This capability facilitated a number of observational modes which considerably enhanced the science return from this mission, including the extension of the latitudinal coverage to ±74°. Details are given below.

[12] The CRISTA measurements cover altitudes from the upper troposphere to the lower thermosphere. This large altitude range is scanned in different scan modes which concentrate either on the troposphere/stratosphere or on the mesosphere/lower thermosphere regions. The scan modes, their altitude coverage, the step width, and the time spent for each mode are summarized in Table 2. Emissions from the lower thermosphere are almost exclusively analyzed by channels of the center telescope spectrometers. During the mesosphere/lower thermosphere scan modes the lateral telescopes' scan pattern is therefore limited in altitude in order to optimize the data return.

[13] Several special observation modes were carried out by CRISTA-2 to test the instrument capabilities for possible

Table 2. Standard Observation Modes

Mode	Altitudes, km Scan Step, km Center Telescope	Altitudes, km Scan Step, km Lateral Telescope	Time
S (stratosphere)	11–55 (SCS) 31–75 (SCL)	11–55	88 h 48 m
	Δz = 2	Δz = 2	
S–L (stratosphere-low)	7–55 (SCS) 27–75 (SCL)	7–55	9 h 25 m
	Δz = 2	Δz = 2	
M (mesosphere)	40–130 (SCS) 60–150 (SCL)	15–105	60 h 27 m
	Δz = 2.15	Δz = 2.15	
T (thermosphere)	60–165 (SCS) 80–185 (SCL)	60–102	22 h 57 m
	Δz = 2.5	Δz = 1	
nadir			1 h 16 m
calibration/alignment			11 h 56 m
		total	194 h 49 m

Table 3. Special Observation Modes

Mode	Altitudes	Remarks
validation	11–67 (87, SCL) [km]	during pointing at rocket probes/balloons
nadir	–	standard scans, 1 orbit
strat/vr	same as standard stratosphere modes {S and S–L}	2 spectra on each altitude step—one with increasing/ one with decreasing wavelength
meso/vr	same as standard mesosphere mode {M}	same as strat/vr
relax	fixed 130 km	fixed wavelegth (63 μm)
staring	fixed altitudes SCS = 30 [km] SR/SL = 17 [km]	observation perpendicular to orbit plane
therox	same as thermosphere	reduced spectral scan (63 μm line only)
coalignment	alignment verification between CRISTA and satellite attitude control	slew of primary mirror and slew of ASTRO-SPAS, fixed wavelength
calibration	calibration target on instrument cover MDA	standard spectral scan

future experiments and for technical/calibration reasons. These special modes are listed in Table 3. In order to evaluate and to possibly improve the performance of the relaxation correction model for the detectors on the basis of the inflight data, the special observations ''strat/vr'', ''meso/vr'', and ''relax'' for the stratosphere, mesosphere, and thermosphere scan modes, respectively, were carried out. In these observations each altitude is observed using two spectral scans with different wavelength scan directions. The differences between the two spectra are due to the temporal behavior of the detectors and should be eliminated by means of the relaxation correction model. Such measurements were carried out for the stratosphere and mesosphere scan modes. A different approach was used in the thermosphere for the far infrared wavelengths, since only one spectral feature (single line at 63 μm from atomic oxygen) is present; in this case the spectrometer scans were stopped at the center of the emission line for some time (10 min) to compare longtime constant radiation exposure of the detector with the standard scan.

[14] The calibration/alignment periods include radiometric calibration using a target located in the CRISTA instrument cover, and line-of-sight verifications using Jupiter as a target. The line-of-sight calibrations were performed twice during the mission (Figure 4). The radiometric calibrations were performed whenever the instrument cover was closed in between alignment measurements and before and after the main data-taking period. In Figure 4 the CRISTA mission timeline is shown. At the beginning of the measurement period the mesosphere and thermosphere were sensed, followed by a 4-day period concentrating on the stratosphere. The higher altitudes were observed again for the last 2.5 days of the measurement period.

3. Observations: Stratosphere and Upper Troposphere

[15] The data conditioning and trace gas retrieval procedures are done in the same way and use the same algorithms as for CRISTA-1 [*Riese et al.*, 1999]. Of course the data reduction is still preliminary and less advanced than for the

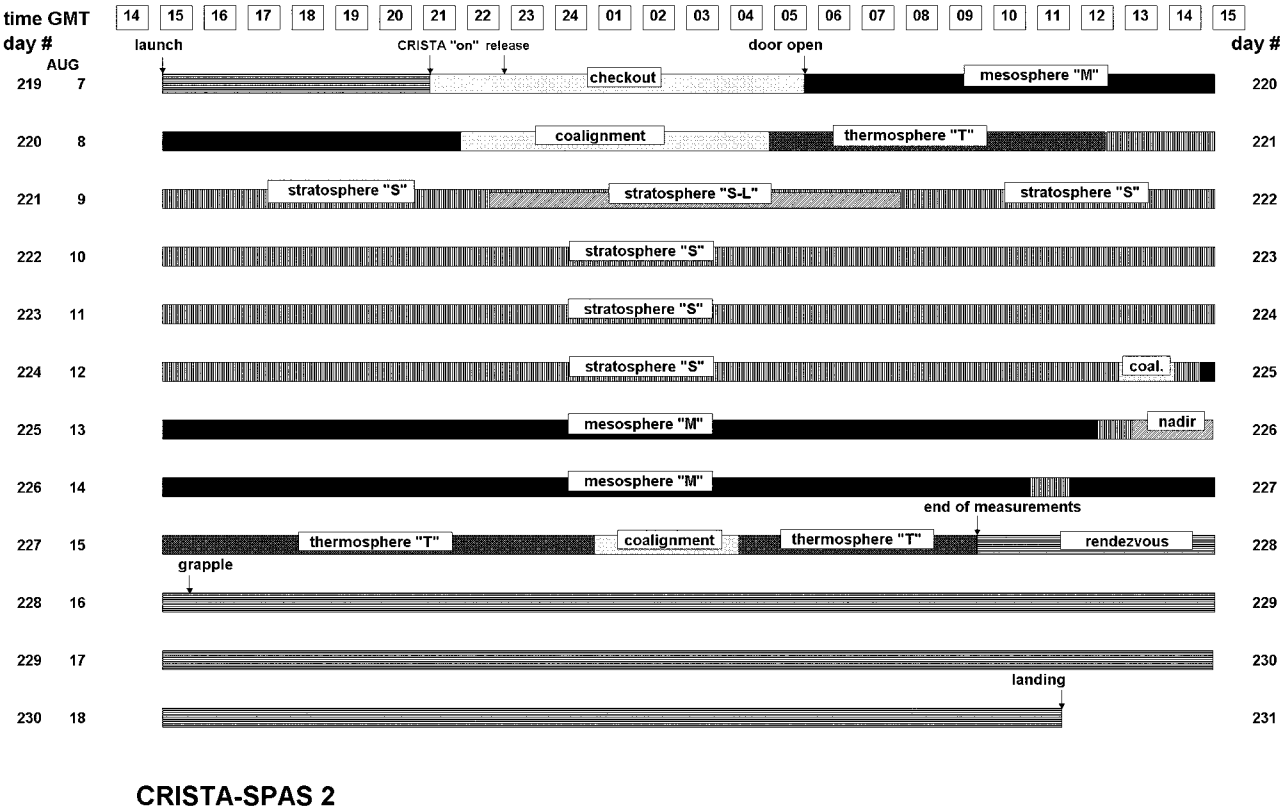

Figure 4. Mission timeline.

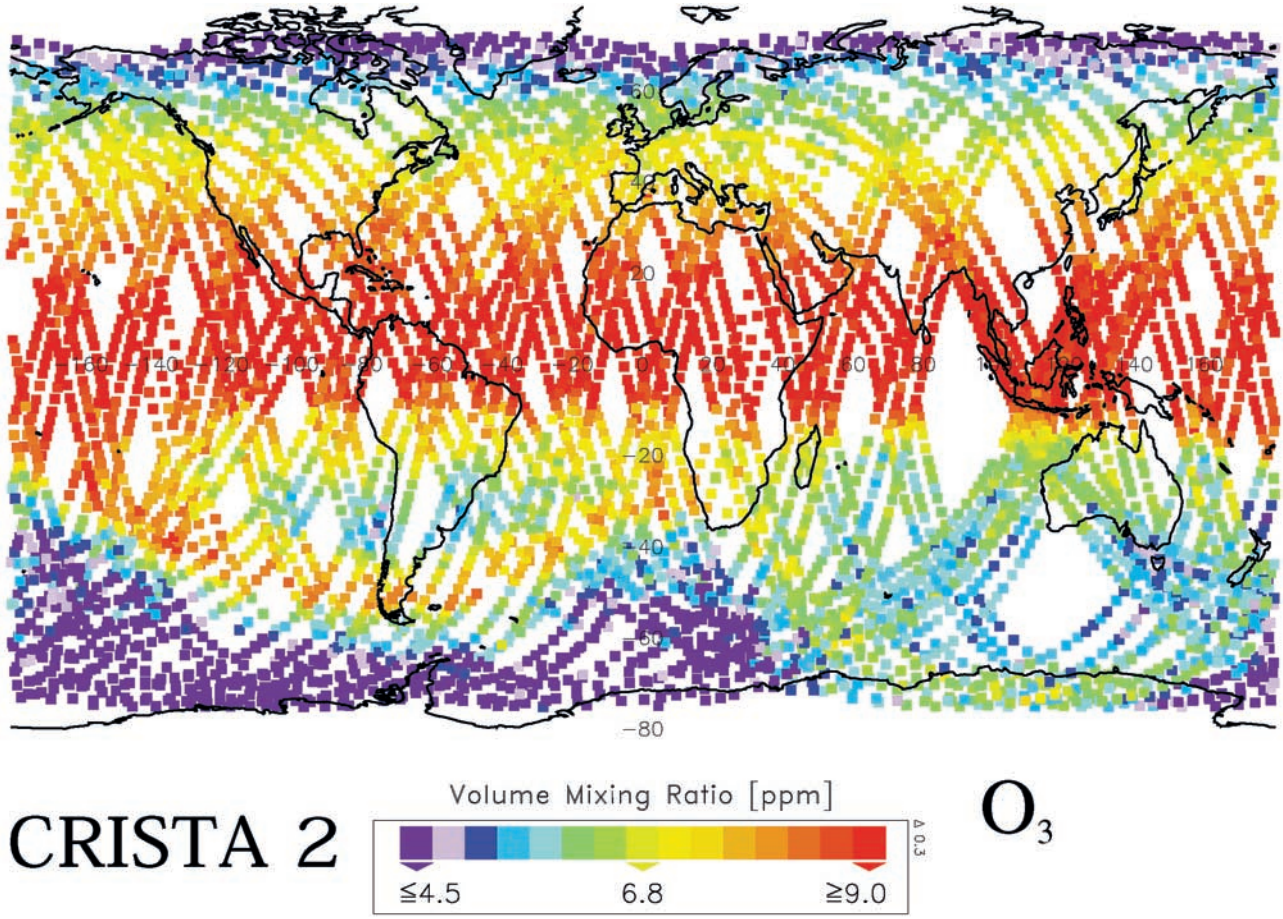

Figure 5. Ozone mixing ratios at 31 km altitude measured on one day.

first mission. The data from CRISTA-2 presented in the various papers of this volume are labeled V1 (version 1). Most of them can be accessed via the CRISTA homepage: http://www.crista.uni-wuppertal.de.

[16] An example of the data from the stratospheric observations (Table 2) is shown in Figure 5. Ozone mixing ratios measured on 10 August 1997 at an altitude of 31 km are presented. The data in Figure 5 were recorded over a period of 24 hours. Each symbol represents one complete altitude scan of all gases measured by CRISTA. The tracks of the three telescopes are clearly seen. Figure 5 demonstrates the amount of soundings and the data density of CRISTA obtained during one day only. Most of this day CRISTA was operated in a standard observation geometry, the so-called ''ping-pong'' mode. In this attitude mode CRISTA-SPAS slews with constant angular velocity alternating clockwise and counterclockwise around the local vertical axis. The movements are synchronized with the orbit position such that the CRISTA center telescope views northwards (or more precisely at +72° from the orbit plane) at the northernmost point of each orbit, views backwards (i.e. within the orbital plane but at 180° to the velocity vector) while above the equator, and views southwards (at −72° from the orbital plane) at the southernmost point of the orbit. The ''L'' telescope is then oriented straight north at the high north orbital position of CRISTA and the ''R'' telescope is oriented straight south at the respective point in the southern hemisphere. As CRISTA is a limb viewing experiment latitudes up to about ±74° are accessible in the stratosphere (Figure 5) although flying on a 57° orbit. At higher altitudes the latitudinal coverage is slightly less.

[17] In the northern summer hemisphere a gradual decrease of the ozone mixing ratios from high concentrations over the tropics to low values at polar latitudes is observed. The longitudinal variations are low as far as large scale structures (i.e. larger than 1500 km) are concerned. In Figure 6a the ozone concentrations at 31 km in the 40–50°N latitude band and averaged over 10° in longitude are plotted. The maximum variability is ±0.2 ppmv or less than 3%. The profile in Figure 6b shows the same quantity but for the southern hemisphere (40–50°S). Considerable large scale wave activity is seen with mixing ratio variations which are higher by a factor of 10 compared to the northern hemisphere [*Ward et al.*, 2000]. The accuracy of the derived mixing ratios is 10% for the northern hemisphere profile and 9% for the southern hemisphere profile. The statistical errors in Figure 6 are below 0.7% and therefore much lower than the observed fluctuations. The dynamical situation of the stratosphere was dominated by strong planetary wave activity in the southern hemisphere [*Günther et al.*, 2002; *Riese et al.*, 2002]. This shows up in form of streamers in the ozone distribution of Figure 5. Similar structures and in a number of trace gases were found by CRISTA-1 [*Offermann et al.*, 1999]. Two streamers of ozone rich air can be identified. One streamer leaves the subtropics over the central pacific, leads over the southern tip of South America, and then goes back

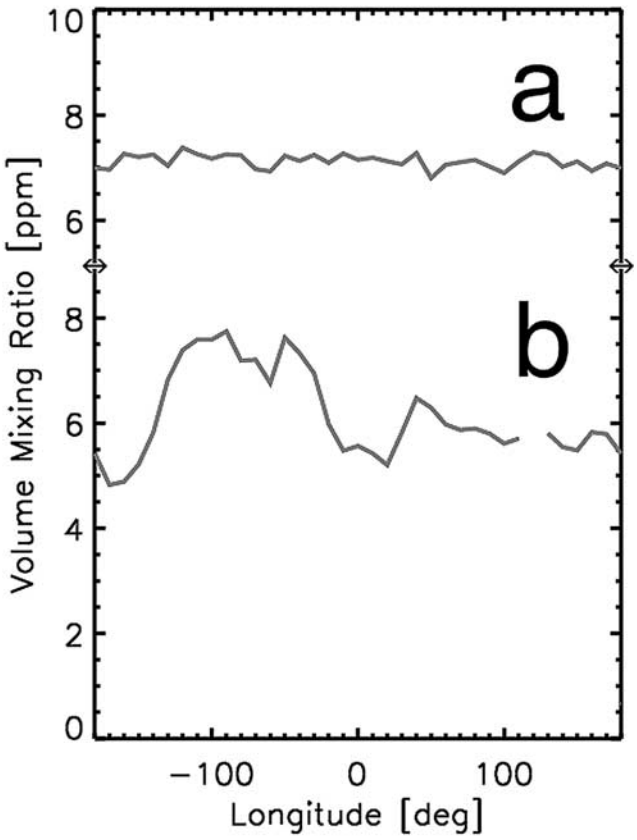

Figure 6. Ozone mixing ratios at 31 km altitude in the northern (a) and southern hemisphere (b). The errors of the two profiles are about 10% systematic. The statistical errors are below 0.7%.

to the subtropics west of southern Africa. The second and weaker one is still in its formation phase and extends from southern Africa to the Antarctic continent south of Australia. The streamers are the result of the shape of the polar vortex which was quite elongated at this time [*Günther et al.*, 2002]. The streamers are also identified in other trace gases [*Küll*, 2002; *Riese et al.*, 2002]. Other observed large-scale disturbances include Kelvin waves [*Smith et al.*, 2002] and tides [*Hagan et al.*, 2002].

[18] A particularly dense measurement net is obtained in the so-called "hawkeye" mode observations which were performed above Indonesia (Figure 5). In this mode CRISTA is pointed toward the same geographical region during three adjacent orbits, thus tripling the local number of air volumes sensed within slightly more than 3 hours. This is possible since the distance from CRISTA to the measurement volume at the tangent point is very similar to the longitudinal orbit separation at low latitudes. Combining ascending and descending orbits further increases the data density at the expense of temporal resolution, however. The "hawkeye" observation geometry of course results in some data gaps over adjacent areas. The average profile distance within the hawkeye region is 165 km if the 3 ascending and the 2 descending orbits are combined [*Grossmann*, 2000]. The maximum time difference between "hawkeye" data points is then about 13 hours. The region chosen for this observation mode is above Indonesia. In this area small scale structures due to the frequently occurring deep convection cells are expected [*Chen and Houze*, 1997]. The occurrence of high reaching clouds is analyzed by *Spang et al.* [2002].

[19] Figure 7 shows two altitude profiles of ozone mixing ratios taken at a distance of only 114 km from each other and within 90 min in the "hawkeye" region. Despite this "good" coincidence the mixing ratios differ by about 0.8 ppmv in the altitude interval 28–32 km. The example given in Figure 7 is typical for most similar pairs. It shows that there is considerable variability at very small scales probably due to waves and/or turbulence. It also shows that validation measurements or joint measurements by a number of sensors are not always meaningful if they are not performed at exactly the same time and in exactly the same volume of air. Such "zero miss-distance/zero miss-time" validations were performed in a comprehensive ground-based, aircraft, balloon, and rocket campaign together with CRISTA-SPAS-2. The aim of this campaign was to validate the satellite measurements and gas retrievals, to monitor the state of the atmosphere before and after the mission, and to determine additional parameters not observed by the space-borne instruments. A total of 43 rockets and 78 balloons were launched between 30 July and 30 August 1997 in addition to measurements from 46 ground stations. The attitude control capabilities of the ASTRO-SPAS were used to point CRISTA to locations into which balloons and/or rockets were launched simultaneously in order to perform near "zero miss-distance/-time" joint measurements. The validation comparison was optimized by setting up an adopted altitude scan pattern (validation mode in Table 3). Temperature comparisons with the data of 10 falling spheres launched from Wallops Island, VA, USA, were possible at an average distance of only 33 km between the falling sphere and the center of the CRISTA sampling volume at zero time difference. Details of these validation measure-

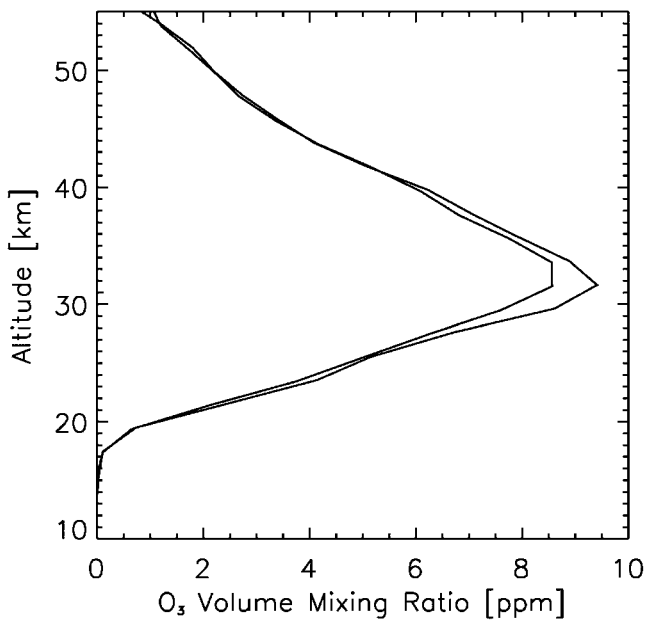

Figure 7. Vertical profiles of ozone mixing ratios taken near 113°E/7°S. The separation between the profiles is 114 km and 90 min.

ments are given by [*Lehmacher et al.*, 2000]. Measurements in common volumes of air were also done by the MAHRSI instrument jointly with a far infrared heterodyne receiver (THOMAS, *T*era *H*ertz *O*H *M*easurement *A*irborne *S*ounder) aboard the DLR Falcon aircraft which flew over central Europe [*Englert et al.*, 2000]. The two instruments observe the concentration of OH radicals at UV wavelengths (MAHRSI) and in the far infrared (THOMAS). The DLR aircraft also carried the Fast In-situ Stratospheric Hygrometer (FISH) instrument [*Zoeger et al.*, 1999]. Upper tropospheric water vapour distributions and their spatial and temporal variabilities are discussed by *Offermann et al.* [2002] together with the results from the FISH experiment.

[20] Small-scale structures are observed in many parameters. *Eidmann et al.* [2002] analyze variabilities of ozone concentrations and temperatures at various scales down to below 100 km. Part of these variations are due to gravity waves which can be extracted from the CRISTA temperature data [*Preusse et al.*, 2002]. Very small spatial scales are examined in a special "staring" mode. In this mode the CRISTA instrument views perpendicular to the orbit plane and no altitude scans are performed. Structures at the spectral scan rate of 1.3 s, translating to a spatial scale of 11.3 km, can be studied. This mode was carried out over one orbit only. A second feature for the study of very small scales is a special detector arrangement in the SCS6 channel (Table 1). This is the only SCS channel which is not equipped with a Si:As BIB detector but has 3 Si:Ga bulk detectors arranged along the spectrometer exit slit. Each of these detectors (labeled SCS6, SCS6R, and SCS6L) views an atmospheric footprint about 6 km wide (as compared to about 20 km for the other detectors of Table 1). Due to limitations in the data conditioning electronics, the detectors SCS6R and SCS6L could only be switched on for 5.3 hours, when channels SCS3 and SCS4 were turned off, whereas the SCS6 detector operated continually. Furthermore, channel SCS6L failed in orbit so that only one detector pair was operable. When observing in the staring mode the two detectors view the same volume of air in less than 1 s. Comparison of the data from the two detectors then allows very small scale structures to be distinguished from noise peaks or other nonatmospheric disturbances. Some data of this special mode have been analyzed to give wave number spectra of the observed fluctuations [*Eidmann et al.*, 2001].

4. Observations: Mesosphere/Lower Thermosphere

[21] During CRISTA-2 a considerable amount of data was gathered in the altitude regime of the upper mesosphere and lower thermosphere (Table 2, Figure 4). In the thermosphere the atomic oxygen fine structure transition $^3P_1 \rightarrow {}^3P_2$ at 63 μm is observed up to about 185 km with the SCL spectrometer. The 63 μm emission is a single line and the oxygen fine structure levels are in local thermodynamic equilibrium (LTE) in the altitude regime considered here. The excitation energy of the upper level ($^3P_1$) is very low (158 cm^{-1}). The emission therefore is only a weak function of the local temperature and model temperatures can be used to derive densities from the measured line intensities. Global atomic oxygen density distributions have been deduced for day and night conditions between 130 km and 175 km and were found about 40% lower [*Grossmann et al.*, 2000] than predicted by the MSISE-90 model [*Hedin*, 1991]. These low oxygen concentrations may have been a result of the rather quiet geophysical conditions near the solar minimum. The solar radio emission flux index (10.7 cm radio flux in units of 10^{-22} $Wm^{-2}Hz^{-1}$) was between $F_{10.7} = 79.6$ and $F_{10.7} = 84.2$. The CRISTA-2 conditions are therefore quite similar to those of the first CRISTA flight in November 1994. Also the geomagnetic activity was rather moderate. The daily averaged A_p (linear planetary geomagnetic activity) index varied between 5 and 8 during most of the mission period and reached 11 and 16 on 13 and 14 August, respectively.

[22] Molecular emissions in the upper mesosphere/lower thermosphere include the 15 μm and the 4.3 μm CO_2 ν_2- and ν_3-bands, the 9.6 μm ozone band, the thermospheric $\Delta\nu = 1$ band of nitric oxide at 5.3 μm, and the 4.7 μm band of carbon monoxide. Compared to CRISTA-1, the data quality was considerably improved here due the use of highly sensitive Si:As BIB detectors in the center telescope midinfrared channels. A spectrum of the SCS2 channel at an altitude of 90 km taken at 70.5°N is shown in Figure 8. The main feature centered at about 2325 cm^{-1}, is caused by the combination of several solar pumped CO_2 ν_3-hot-bands. The shoulders near 2370 cm^{-1} and near 2275 cm^{-1} are caused by part of the fundamental bands of the main isotope $C^{12}O^{16}O^{16}$ and the $C^{13}O^{16}O^{16}$ isotope, respectively. At lower wave numbers (2080–2200 cm^{-1}) the $\Delta\nu = 1$ vibration-rotation band of carbon monoxide (CO) is well displayed. The noise equivalent spectral radiance of this channel is $1.9 \cdot 10^{-11}$ $Wcm^{-2}sr^{-1}(cm^{-1})^{-1}$. The spectral resolution is 5.5 cm^{-1}.

[23] The molecular emissions stem from energy levels which are not in local thermodynamic equilibrium (non-LTE). Under these conditions the infrared radiation emitted by the molecules is no longer a function of the local temperature alone. All relevant excitation and quenching processes by collisional as well as by radiative interaction have to be explicitly modeled [*Gordiets et al.*, 1982; *Dickinson*, 1984]. In the midinfrared domain of molecular vibration–rotation bands in general a huge number of different energy levels must be treated simultaneously. As a consequence the computational effort is quite high. Furthermore, many of the non-LTE model derived parameters (CO_2, atomic oxygen, and ozone densities, kinetic temperatures, and radiation fields) are interlinked such that these parameters have to be retrieved in a self consistent way. The general approach to the solution of this problem was described by *Grossmann et al.* [2002]. The non-LTE model [*Kutepov et al.*, 1998] can be applied to the analysis of a number of different non-LTE emissions. The specific applications for the CO_2 emissions are given by *Ogibalov et al.* [1998] and *Shved et al.* [1998] and for ozone by *Manuilova et al.* [1998]. So far, CO_2 and O_3 densities were retrieved for both CRISTA-1 and CRISTA-2. The CO_2 densities are for daytime and show considerable latitudinal and longitudinal variations [*Kaufmann et al.*, 2002]. De-mixing of CO_2 begins at 75–80 km in contrast to current model predictions but in agreement with analyses by *López-Puertas et al.* [2000]. Ozone densities were derived for day- and nighttime up to above 90 km [*Kaufmann et al.*, 2000]. These data show high ozone concentrations at the secondary ozone maximum in the lower thermosphere and a third local ozone maximum

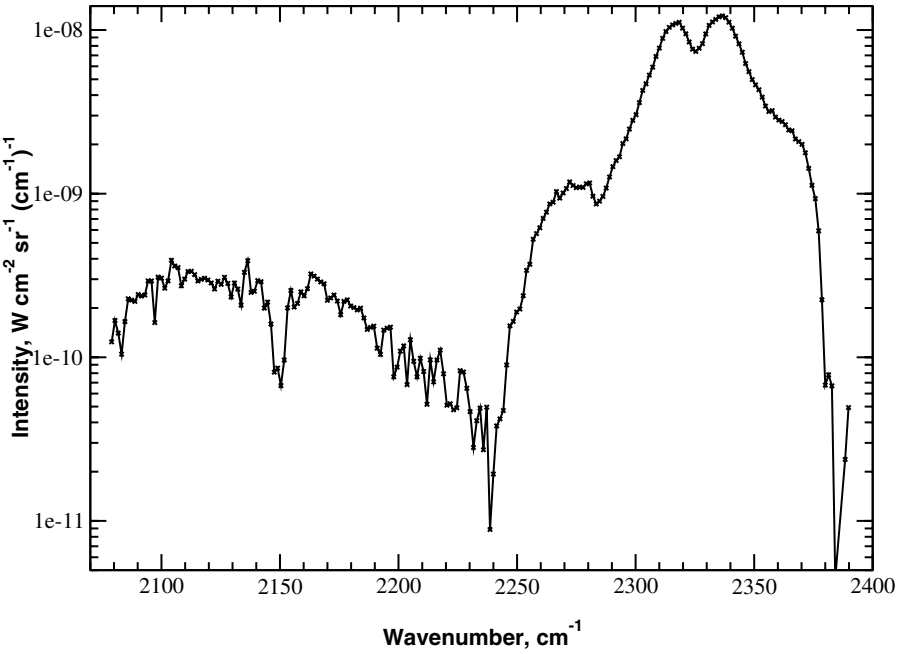

Figure 8. Sample spectrum of channel SCS-2 at a tangent altitude of 90 km.

near the high latitude terminator in the winter hemisphere [*Marsh et al.*, 2001].

[24] Atmospheric temperatures are usually derived from the analysis of emissions in the CO_2 v_2-band (15 μm band) [*Kennedy and Nordberg*, 1967; *Gille and House*, 1971]. In the upper mesosphere, the difference between the LTE and the non-LTE populations of the CO_2 v_2-levels which is equivalent to the difference between the kinetic and the vibrational temperatures, is not very large for high mesopause temperatures. *López-Puertas et al.* [1992] deduced differences of only a few K up to 100 km from ATMOS/Spacelab 3 observations at springtime midlatitudes. At low temperatures during high-latitude summer the differences increase considerably as temperature gradients in the atmosphere increase and nonlocal radiative pumping becomes more effective [*Ratkowski et al.*, 1994]. A test of a non-LTE model is therefore particularly meaningful under these low temperature conditions.

[25] Temperature profiles (>300) derived from the spectra of the SCL2 channel (Table 1) are shown in Figure 9. All profiles were taken at latitudes above 65°N during the mesosphere modes (Table 2). Mesopause temperatures between 130 and 155 K are inferred in most cases. Considerable wave

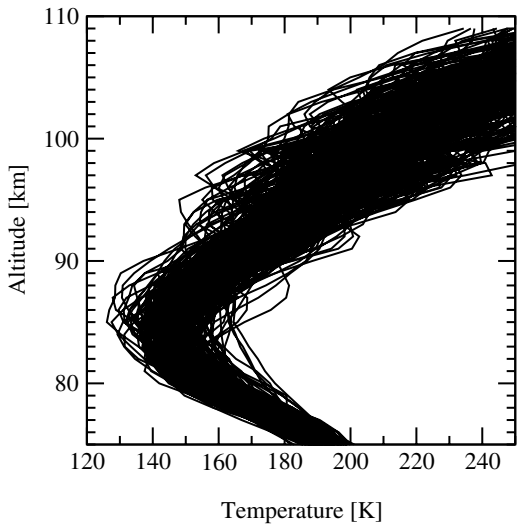

Figure 9. Temperature profiles (>300) taken at latitudes above 65°N.

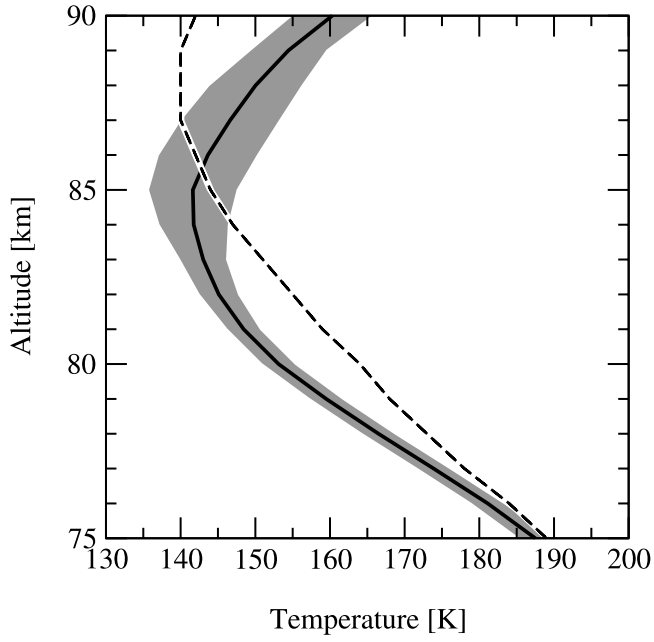

Figure 10. Mean temperature for latitudes >65°N and from the climatology of *Lübken* [1999]. The shaded area gives the error limits of the CRISTA derived temperatures. For details see text.

activity is present in the data set. The mean temperature averaged over all profiles of Figure 9 is given in Figure 10. The mesopause in the mean profile is at 141.6 K and at an altitude of 85 km (±0.7 km). The standard CRISTA temperature retrieval for the stratosphere and mesosphere assumes LTE at all altitudes [*Riese et al.*, 1999]. These ''LTE-temperatures'' are calculated up to altitudes of 90 km and can therefore be compared directly to the non-LTE model inferred temperatures. For latitudes >65° and on 13 August the mean ''LTE-temperature'' at 85 km is 171 K. The large difference of near 30 K under the high latitude summer conditions is an extreme case for the atmosphere but it underlines the importance of the non-LTE modeling. At medium and low latitudes as well as in the winter hemisphere the differences are much smaller. The LTE temperatures have been used to derive geostrophic wind fields in the stratosphere and mesosphere which compare well with other measurements at mid and low latitudes [*Oberheide et al.*, 2002]. The winds at high summer latitudes have to be reanalyzed on the basis of the non-LTE temperatures. The present accuracy of the non-LTE temperature retrieval is dominated by two error sources—(a) the rate at which CO_2 is quenched by atomic oxygen and (b) the errors of the CO_2 density retrieval as given by [*Kaufmann et al.*, 2002]. The $O(^3P)-CO_2$ (v_2) quenching rate has been a matter of debate since long [*Sharma and Wintersteiner*, 1990; *López-Puertas et al.*, 1998] and a factor of 2 uncertainty is assumed. In addition there are errors due to the accuracy of the derived $O(^3P)$ densities which comes from the non-LTE ozone retrieval and from the fact that the derivation of $O(^3P)$ from ozone was not yet iterated with the retrieved non-LTE temperatures. The errors due to calibration, noise, and CO_2 line parameters are small in comparison but become important below about 82 km. The systematic errors are included in Figure 10 (shaded area) and reach a maximum of ±6.4 K at 87 km.

[26] A climatology of high latitude summer mesosphere temperatures was derived by *Lübken* [1999] from the data of falling sphere soundings over northern Scandinavia (69°N). The results of *Lübken* for mid-August are included in Figure 10. The two profiles generally agree reasonably well taking the combined error bars into account (Lübken states uncertainties of 7 K and 3 K at 90 km and 80 km, respectively). In the CRISTA data the mesopause is at about the same temperature but is about 3 km lower than in the Lübken analysis. Toward higher altitudes there is an increasing discrepancy between the CRISTA remote sensing temperatures and the falling sphere derived ones which needs future clarification. Higher up in the thermosphere, however, the CRISTA temperatures agree well with the model temperatures of MSIS [*Grossmann et al.*, 2002]. The variability among the CRISTA profiles (Figure 9) is very similar to the variability given by Lübken for 23 summer profiles.

[27] The mesopause altitude determined from the high latitude profiles is 85 km for an average latitude of 69°N. The average mesopause in the low latitude soundings (<40°N) and in the winter hemisphere is located at 98 km. This is consistent with the split mesopause phenomenon described by *von Zahn et al.* [1996] and analyzed by *Berger and von Zahn* [1999].

[28] Low mesopause temperatures as those of Figure 10 can lead to the formation of polar mesospheric clouds (PMCs) or noctilucent clouds (NLCs). PMCs have been studied by many observers from the ground, by sounding rockets, or from satellites [*Gadsden and Schroeder*, 1989]. Both CRISTA and MAHRSI detected PMC signatures in the infrared and ultraviolet part of the spectrum [*Stevens et al.*, 2001].

5. Summary

[29] The CRISTA-2 mission yielded a wealth of data about highly resolved trace gas distributions in August 1997. The dense measurement grid of the triple beam limb sounder obtained during the first mission in November 1994 was extended in latitudinal coverage to ±74° based on the satellite capability to maneuver in space while maintaining all three CRISTA beams simultaneously at the Earth limb. The mission took place during a period of very strong planetary wave activity. Streamers are observed in several trace gases in the stratosphere as was the case during the first CRISTA mission. A special high spatial density observation mode (''hawkeye'') was executed in the region over Indonesia. From ozone density data recorded in this mode as well as from fluctuation analyses of other parameters and over other areas it can be concluded that the trace gas concentrations vary considerably over very short distances. For the same reason zero miss-distance/-time validation measurements were done for CRISTA-2 by pointing the instrument to simultaneously launched rockets, balloons, or to an aircraft.

[30] The altitude regime covered by the CRISTA measurements was increased to include the upper troposphere. Water vapor concentrations were derived and exhibit considerable structures over very short spatial scales. More time was allocated to the upper mesosphere and the lower thermosphere and a comprehensive data set was collected here. As at these altitudes non-LTE modeling is required to retrieve atmospheric parameters the data have only been partially evaluated as yet. Atomic oxygen densities in the thermosphere and carbon dioxide and ozone densities in the upper mesosphere and lower thermosphere have been derived. The first summer high latitude mesopause region temperatures from 15 μm band spectra are found to agree well with a climatology based on falling sphere data.

[31] The results presented in the set of papers in this issue show how variable the atmosphere is at all altitudes and in all parameters. The analyses will be continued and refined in the next future.

[32] **Acknowledgments.** The success of the CRISTA-2 experiment would not have been possible without the support by a large number of individuals and institutions. We would particularly like to thank the teams at NASA-HQ, -JSC, and -KSC for the very fruitful cooperation and for their unbureaucratic consideration of our special wishes. Special thanks go to the team of Konrad Moritz at DASA, München, for their outstanding personal efforts to bring CRISTA and MAHRSI to a full success. CRISTA-2 was supported by DARA/DLR, Bonn, through grants 50 QV 9501 and 50 QV 9802.

References

Baldwin, M. P., and T. J. Dunkerton, Propagation of the arctic oscillation from the stratosphere to the troposphere, *J. Geophys. Res.*, *104*, 30,937–30,946, 1999.

Baldwin, M. P., and T. J. Dunkerton, Propagation of annular modes from the mesosphere to the Earth's surface, paper presented at 2nd SPARC General Assembly, Mar del Plata, Argentina, 6–10 November 2000.

Beig, G., The relative importance of solar activity and anthropogenic influences on the ion composition, temperature, and associated neutrals of the middle atmosphere, *J. Geophys. Res.*, *105*, 19,841–19,856, 2000.

Berger, U., and U. von Zahn, The two-level structure of the mesopause: A model study, *J. Geophys. Res.*, *104*, 22,083–22,093, 1999.

Chen, P., J. R. Holton, A. O'Neill, and R. Swinbank, Isentropic mass exchange between the tropics and the extratropics in the stratosphere, *J. Atmos. Sci.*, *51*, 3006–3018, 1994.

Chen, S. S., and R. A. Houze Jr., Interannual variability of deep convection over the tropical warm pool, *J. Geophys. Res.*, *102*, 25,783–25,796, 1997.

Conway, R. R., M. H. Stevens, C. M. Brown, J. G. Cardon, S. E. Zasadil, and G. H. Mount, Middle Atmosphere High Resolution Spectrograph Investigation, *J. Geophys. Res.*, *104*, 16,327–16,348, 1999.

Crutzen, P., Mesospheric mysteries, *Science*, *277*, 1951–1952, 1997.

Dickinson, R. E., Infrared radiative cooling in the mesosphere and lower thermosphere, *J. Atmos. Terr. Phys.*, *46*, 995–1008, 1984.

Drummond, J. R., J. T. Houghton, G. D. Peskett, C. D. Rodgers, M. J. Wale, J. Whitney, and E. J. Williamson, The stratospheric and mesospheric sounder on Nimbus 7, *Phil. Trans. R. Soc. London, Ser. A*, *296*, 219–241, 1980.

Eckermann, S. D., and P. Preusse, Global measurements of stratospheric mountain waves from Space, *Science*, *286*, 1534–1537, 1999.

Edwards, D. P., G. Zaragoza, M. Riese, and M. López-Puertas, Evidence of H_2O non-local thermodynamic equilibrium emission near 6.4 μm as measured by CRISTA-1, *J. Geophys. Res.*, *105*, 29,003–29,022, 2000.

Eidmann, G., D. Offermann, and P. Preusse, Fluctuation power spectra in the mid stratosphere at increased horizontal resolution, *Adv. Space Res.*, *27*, 1647–1652, 2001.

Eidmann, G., D. Offermann, B. Schaeler, M. Jarisch, and F. J. Schmidlin, Stratospheric variability of temperature and ozone as inferred from the second CRISTA mission, 1, Zonal means and local structures, *J. Geophys. Res.*, *107*, 10.1029/2001JD000721, 2002.

Englert, C. R., B. A. Schimpf, M. Birk, F. Schreier, R. R. Conway, M. H. Stevens, and M. E. Summers, THOMAS 2.5 THz measurements of middle atmospheric OH: Comparison with MAHRSI observations and model results, in *Atmospheric Science Across the Stratopause*, edited by D. E. Siskind, S. D. Eckermann, and M. E. Summers, *Geophys. Monogr.*, vol. 103, pp. 305–310, 2000.

Ern, M., K. U. Grossmann, and D. Offermann, Detector signal relaxations and their correction: The Si:Ga bulk detectors of the CRISTA instrument, *Proc. SPIE Int. Soc. Opt. Eng.*, *4486*, 111–121, 2002.

Gadsden, M., The secular change in noctilucent cloud occurrence: Study of a 31-year sequence to clarify the causes, *Adv. Space Res.*, *20*, 2097–2100, 1997.

Gadsden, M., and W. Schroeder, *Noctilucent Clouds, Physics and Chemistry in Space Planetology*, vol. 18, Springer-Verlag, New York, 1989.

Gille, J. C., and F. B. House, On the inversion of limb radiance measurements, 1, Temperature and thickness, *J. Atmos. Sci.*, *28*, 1427–1442, 1971.

Gille, J. C., and J. M. Russell III, The limb infrared monitor of the stratosphere: Experiment description, performance, and results, *J. Geophys. Res.*, *89*, 5125–5140, 1984.

Gordiets, B. F., Yu. N. Kulikov, M. N. Markov, and M. Ya. Marov, Numerical modeling of the thermospheric heat budget, *J. Geophys. Res.*, *87*, 4504–4514, 1982.

Grossmann, K. U., Recent improvements in middle atmospheric remote sounding techniques: The CRISTA-SPAS experiment, in *Atmospheric Science Across the Stratopause*, edited by D. E. Siskind, S. D. Eckermann, and M. E. Summers, *Geophys. Monogr.*, vol. 103, pp. 287–304, 2000.

Grossmann, K. U., and D. Offermann, 2. Flug von CRISTA, *Tech. Rep. 50 QV 9501*, Univ. Wuppertal, Wuppertal, Germany, 1999.

Grossmann, K. U., M. Kaufmann, and E. Gerstner, A global measurement of lower thermosphere atomic oxygen densities, *Geophys. Res. Lett.*, *27*, 1387–1390, 2000.

Grossmann, K. U., O. Gusev, M. Kaufmann, and A. A. Kutepov, Atmospheric parameters retrieved from CRISTA measurements in the upper mesosphere and lower thermosphere, *Proc. SPIE Int. Soc. Opt. Eng.*, 4539, 406–417, 2002.

Günther, G., D. S. McKenna, and R. Spang, The meteorological conditions of the stratosphere for the CRISTA/MAHRSI-2 campaign (July/August 1997), *J. Geophys. Res.*, *107*, 10.1029/2001JD000692, in press, 2002.

Hagan, M. E., R. G. Roble, C. Hartsough, J. Oberheide, and M. Jarisch, The dynamics of the middle atmosphere during CRISTA-2 as simulated by the NCAR TIME-GCM, *J. Geophys. Res.*, *107*, 10.1029/2001JD000679, in press, 2002.

Haynes, P. H., On the "downward control" of extratropical diabatic circulation by eddy-induced mean zonal forces, *J. Atmos. Sci.*, *48*, 651–678, 1991.

Hedin, A. E., Extension of the MSIS thermosphere model into the middle and lower atmosphere, *J. Geophys. Res.*, *96*, 1159–1172, 1991.

Kaufmann, M., R. R. Garcia, K. U. Grossmann, O. Gusev, L. Knuefing, and A. A. Kutepov, The global distribution of O_3 in the mesosphere measured by CRISTA, paper presented at 33rd COSPAR Scientific Assembly, Warsaw, 16–23 July 2000.

Kaufmann, M., O. A. Gusev, K. U. Grossmann, R. G. Roble, M. E. Hagan, and C. Hartsough, The global distribution of CO2 densities in the upper mesosphere and lower thermosphere during CRISTA, *J. Geophys. Res.*, *107*, 10.1029/2001JD000704, in press, 2002.

Kaye, J. A., and T. L. Miller, The ATLAS series of shuttle missions, *Geophys. Res. Lett.*, *23*, 2285–2288, 1996.

Kennedy, J. S., and W. Nordberg, Circulation features of the stratosphere derived from radiometric temperature measurements with the TIROS VII satellite, *J. Atmos. Sci.*, *24*, 711–719, 1967.

Krueger, A. J., B. Guenther, A. J. Fleig, D. F. Heath, E. Hilsenrath, R. McPeters, and C. Prabhakara, Satellite ozone measurements, *Phil. Trans. R. Soc. London, Ser. A*, *296*, 191–204, 1980.

Küll, V., M. Riese, X. Tie, T. Wiemert, G. Eidmann, D. Offermann, and G. Brasseur, NO_y partitioning and aerosol influences in the stratospheres, *J. Geophys. Res.*, *107*, doi:10.1029/2001JD001246, in press, 2002.

Kutepov, A. A., O. A. Gusev, and V. P. Ogibalov, Solution of the non-LTE problem for molecular gas in planetary atmospheres: Superiority of accelerated lambda iteration, *J. Quant. Spectrosc. Radiat. Transfer*, *60*, 199–220, 1998.

Lehmacher, G. A., J. Oberheide, F. J. Schmidlin, and D. Offermann, Zero miss time and zero miss distance experiments for validation of CRISTA 2 temperatures, *Adv. Space Res.*, *26*, 965–969, 2000.

López-Puertas, M., M. Á. López-Valverde, C. P. Rinsland, and M. R. Gunson, Analysis of the upper atmosphere CO_2 (v_2) vibrational temperatures retrieved from ATMOS/Spacelab 3 observations, *J. Geophys. Res.*, *97*, 2469–2478, 1992.

López-Puertas, M., G. Zaragoza, and M. Á. López-Valverde, Non local thermodynamic equilibrium (LTE) atmospheric limb emission at 4.6 μm 1. An update of the CO_2 non-LTE radiative transfer model, *J. Geophys. Res.*, *103*, 8499–8513, 1998.

López-Puertas, M., M. A. López-Valverde, R. R. Garcia, and R. G. Roble, Review of CO_2 and CO abundances in the middle atmosphere, in *Atmospheric Science Across the Stratopause*, edited by D. E. Siskind, S. D. Eckermann, and M. E. Summers, *Geophys. Monogr.*, vol. 103, pp. 83–100, 2000.

Lübken, F.-J., Thermal structure of the arctic summer mesosphere, *J. Geophys. Res.*, *104*, 9135–9149, 1999.

Manuilova, R. O., et al., Modelling of non-LTE limb spectra of i.r. ozone bands for the MIPAS space experiment, *J. Quant. Spectrosc. Radiat. Transfer*, *59*, 405–422, 1998.

Marsh, D. R., A. K. Smith, G. P. Brasseur, M. Kaufmann, and K. U. Grossmann, The existence of a tertiary ozone maximum in the high-latitude middle atmosphere, *Geophys. Res. Lett.*, *28*, 4531–4534, 2001.

McIntyre, M. E., and T. N. Palmer, Breaking planetary waves in the stratosphere, *Nature*, *305*, 593–600, 1983.

Murphy, D. M., D. W. Fahey, M. H. Proffitt, S. C. Liu, K. R. Chan, C. S. Eubank, S. R. Kawa, and K. K. Kelly, Reactive nitrogen and its correlation with ozone in the lower stratosphere and the upper troposphere, *J. Geophys. Res.*, *98*, 8751–8773, 1993.

Oberheide, J., M. E. Hagan, W. E. Ward, M. Riese, and D. Offermann, Modeling the diurnal tide for the Cryogenic Infrared Spectrometers and Telescopes for the Atmosphere (CRISTA) 1 time period, *J. Geophys. Res.*, *105*, 24,917–24,929, 2000.

Oberheide, J., G. A. Lehmacher, D. Offermann, K. U. Grossmann, A. H. Manson, C. E. Meek, F. J. Schmidlin, W. Singer, P. Hoffmann, and R. A. Vincent, Geostrophic wind fields in the stratosphere and mesosphere from satellite data, *J. Geophys. Res.*, *107*, 10.1029/2001JD000655, in press, 2002.

Offermann, D., The MAP/GLOBUS campaign 1983: Introduction, *Planet. Space Sci.*, *35*, 515–524, 1987.

Offermann, D., and R. R. Conway, Preface: Middle atmosphere structures measured by the CRISTA and MAHRSI experiements, *J. Geophys. Res.*, *104*, 16,309–16,310, 1999.

Offermann, D., K. U. Grossmann, P. Barthol, P. Knieling, M. Riese, and R. Trant, Cryogenic Infrared Spectrometers and Telescopes for the Atmosphere (CRISTA) experiment and middle atmosphere variability, *J. Geophys. Res.*, *104*, 16,311–16,325, 1999.

Offermann, D., B. Schaeler, M. Riese, M. Langfermann, M. Jarisch, G. Eidmann, C. Schiller, H. G. J. Smit, and W. G. Read, Water vapor at the tropopause during the CRISTA 2 mission, *J. Geophys. Res.*, *107*, 10.1029/2001JD000700, in press, 2002.

Ogibalov, V. P., A. A. Kutepov, and G. M. Shved, Non-local thermodynamic equilibrium in CO_2 in the middle atmosphere, 2, Populations in the

v1 v2 mode manifold states, *J. Atmos. Sol. Terr. Phys.*, *60*, 315–329, 1998.

Pfister, L., K. R. Chan, T. P. Bui, S. Bowen, M. Legg, B. Gary, K. Kelly, M. Proffitt, and W. Starr, Gravity waves generated by a tropical cyclone during the STEP tropical field program: A case study, *J. Geophys. Res.*, *98*, 8611–8638, 1993.

Preusse, P., S. D. Eckermann, and D. Offermann, Comparison of global distributions of zonal-mean gravity wave variance inferred from different satellite instruments, *Geophys. Res. Lett.*, *27*, 3877–3880, 2000.

Preusse, P., A. Dörnbrack, S. D. Eckermann, M. Riese, B. Schaeler, J. Bacmeister, D. Broutman, and K. U. Grossmann, Space based measurements of stratospheric mountain waves by CRISTA, 1, Sensitivity, method and a case study, *J. Geophys. Res.*, *107*, 10.1029/2001JD000699, in press, 2002.

Randel, W. J., J. C. Gille, A. E. Roche, J. B. Kumer, J. L. Mergenthaler, J. W. Waters, E. F. Fishbein, and W. A. Lahoz, Stratospheric transport from the tropics to middle latitudes by planetary-wave mixing, *Nature*, *365*, 533–535, 1993.

Ratkowski, A. J., R. H. Picard, J. R. Winick, K. U. Grossmann, D. Homann, J. C. Ulwick, and A. J. Paboojian, Lower-thermospheric infra-red emissions from minor species during high-latitude twilight, 2, Analysis of 15 μm emission and comparison with non-LTE models, *J. Atmos. Sol. Terr. Phys.*, *56*, 1899–1914, 1994.

Reynolds, D. B., D. H. Seib, S. B. Stetson, T. Herter, N. Rowlands, and J. Schoenwald, Blocked impurity band hybrid infrared focal plane arrays for astronomy, *IEEE Trans. Nucl. Sci.*, *36*, 857–862, 1989.

Riese, M., R. Spang, P. Preusse, M. Ern, M. Jarisch, D. Offermann, and K. U. Grossmann, Cryogenic Infrared Spectrometers and Telescopes for the Atmosphere (CRISTA) data processing and atmospheric temperature and trace gas retrieval, *J. Geophys. Res.*, *104*, 16,349–16,367, 1999.

Riese, M., V. Küll, X. Tie, G. Brasseur, D. Offermann, G. Lehmacher, and A. Franzen, Modeling of nitrogen species measured by CRISTA, *Geophys. Res. Lett.*, *27*, 2221–2224, 2000.

Riese, M., A. Franzen, X. Tie, and D. Offermann, Tracer structures in the southern hemisphere middle stratosphere observed by CRISTA-1, *Adv. Space Res.*, *27*, 1623–1628, 2001.

Riese, M., G. L. Manney, J. Oberheide, X. Tie, V. Küll, and D. Offermann, Stratospheric transport by planetary wave mixing as observed during CRISTA 2, *J. Geophys. Res.*, *107*, 10.1029/2001JD000629, in press, 2002.

Sharma, R. D., and P. P. Wintersteiner, Role of carbon dioxide in cooling planetary thermospheres, *Geophys. Res. Lett.*, *17*, 2201–2204, 1990.

Shved, G. M., A. A. Kutepov, and V. P. Ogibalov, Non-local thermodynamic equilibrium in CO_2 in the middle atmosphere, I, Input data and populations of the v3 mode manifold states, *J. Atmos. Sol. Terr. Phys.*, *60*, 289–314, 1998.

Smith, A. K., P. Preusse, and J. Oberheide, Middle atmosphere Kelvin waves observed in CRISTA 1 and 2 temperature and trace species, *J. Geophys. Res.*, *107*, 10.1029/2001JD000577, in press, 2002.

Spang, R., M. Riese, and D. Offermann, CRISTA-2 observations of the south polar vortex in winter 1997: A new dataset for polar process studies, *Geophys. Res. Lett.*, *28*, 3159–3162, 2001.

Spang, R., G. Eidmann, D. Offermann, P. Preusse, L. Pfister, and P.-H. Wang, CRISTA observations of cirrus clouds around the tropopause, *J. Geophys. Res.*, *107*, 10.1029/2001JD000698, in press, 2002.

Stevens, M. H., R. R. Conway, C. R. Englert, M. E. Summers, K. U. Grossmann, and O. A. Gusev, PMCs and the water frost point in the Arctic summer mesosphere, *Geophys. Res. Lett.*, *28*, 4449–4452, 2001.

Tan, K. A., and S. Eckermann, Numerical simulations of mountain waves in the middle atmosphere over the Southern Andes, in *Atmospheric Science Across the Stratopause*, edited by D. E. Siskind, S. D. Eckermann, and M. E. Summers, *Geophys. Monogr.*, vol. 103, pp. 311–318, 2000.

Thrane, E. V., T. A. Blix, U.-P. Hoppe, F. J. Lübken, W. Hillert, G. Lehmacher, and D. C. Fritts, A study of small-scale waves and turbulence in the mesosphere using simultaneous in situ observations of neutral gas and plasma fluctuations, *J. Atmos. Sol. Terr. Phys.*, *56*, 1797–1808, 1994.

von Zahn, U., J. Höffner, V. Eska, and M. Alpers, The mesopause altitude: Only two distinctive levels worldwide?, *Geophys. Res. Lett.*, *23*, 3231–3234, 1996.

Ward, W. E., J. Oberheide, M. Riese, P. Preusse, and D. Offermann, Planetary wave two signatures in CRISTA 2 ozone and temperature data, in *Atmospheric Science Across the Stratopause*, edited by D. E. Siskind, S. D. Eckermann, and M. E. Summers, *Geophys. Monogr.*, vol. 103, pp. 319–325, 2000.

Wattenbach, R., and K. Moritz, Astronomical Shuttle Pallet Satellite (ASTRO-SPAS), *Acta Astronaut.*, *40*, 723–732, 1997.

Zoeger, M., et al., Fast in situ stratospheric hygrometers: A new family of balloon-borne and airborne Lyman-α photofragment fluorescence hygrometers, *J. Geophys. Res.*, *104*, 1807–1816, 1999.

K. U. Grossmann, O. Gusev, J. Oberheide, D. Offermann, M. Riese, and R. Spang, Department of Physics, University of Wuppertal, 42097 Wuppertal, Germany. (gross@wpos2.physik.uni-wupertal.de)